

The Bonding Nature and Low-Dimensional Magnetic Properties of Layered Mixed Cu(II)-Ni(II) Hydroxy Double Salts

Seong-Hun Park[†] and Young-Duk Huh^{*}

Department of Chemistry, Institute of Nanosensor and Biotechnology, Dankook University, Gyeonggi-Do 448-701, Korea

^{*}E-mail: ydhuh@dankook.ac.kr

[†]Department of Chemistry, Faculty of Liberal Art and Teacher Education, University of Seoul, Seoul 130-743, Korea

Received October 26, 2012, Accepted December 4, 2012

Layered mixed metal hydroxy double salts (HDS) with the formulas $(\text{Cu}_{0.75}\text{Ni}_{0.25})_2(\text{OH})_3\text{NO}_3$ ((Cu, Ni)-HDS) and $\text{Cu}_2(\text{OH})_3\text{NO}_3$ ((Cu, Cu)-HDS) were prepared *via* slow hydrolysis reactions of CuO with $\text{Ni}(\text{NO}_3)_2$ and $\text{Cu}(\text{NO}_3)_2$, respectively. The crystal structures, morphologies, bonding natures, and magnetic properties of (Cu, Ni)-HDS and (Cu, Cu)-HDS were characterized with X-ray diffraction (XRD), scanning electron microscopy (SEM), Fourier transformation infrared spectroscopy (FT-IR), thermogravimetric analysis (TGA), and a superconducting quantum interference device (SQUID). Even though (Cu, Ni)-HDS has a similar layered structure to that of (Cu, Cu)-HDS, the bonding nature of (Cu, Ni)-HDS is slightly different from that of (Cu, Cu)-HDS. Therefore, the magnetic properties of (Cu, Ni)-HDS are significantly different from those of (Cu, Cu)-HDS. The origin of the abnormal magnetic properties of (Cu, Ni)-HDS can be explained in terms of the bonding natures of the interlayer and intralayer structures.

Key Words : Layered mixed hydroxy double salt, Crystal structures, Magnetic properties

Introduction

Transition metal hydroxides have attracted much interest because of their wide variety of applications as ion exchangers, catalysts, and hosts in intercalation compounds.¹ These materials have also been used as precursors for the fabrication of one-dimensional nanostructures.² The magnetic properties of layered transition metal hydroxide systems have been extensively scrutinized because such materials are thought to be good examples of two-dimensional (2D) magnetic systems.³ These structures have played a significant role in the development of our understanding of low-dimensional magnetic systems. The 2D character of these compounds arises mainly from the dominant exchange interactions within the inorganic layers and from the comparatively small but non-negligible interactions between the inorganic layers.

Layered hydroxy double salts (HDS), $\text{M}_2(\text{OH})_3\text{X}$ ($\text{M} = \text{Cu, Co, Ni}$; $\text{X} = \text{NO}_3^-, \text{CH}_3\text{COO}^-$), have gained particular attention because of their predicted 2D triangular frustration systems.⁴ As a result, magnetic studies have focused on the fabrication of inorganic-organic hybrid systems with large interlayer spacings, such as *n*-alkyl carboxylate, sulfate or sulfonate, which are necessary for blocking the interlayer magnetic interactions.⁵ In our previous studies, we concluded that the magnetic behaviors of inorganic-organic hybrid HDS systems are mainly governed by the pathways of the inorganic magnetic network but that they are also finely controlled by the anchoring groups of the organic anion. Recently, magnetic frustration in HDS systems has been reinvestigated through the introduction of non-magnetic Zn^{2+} ions into the copper layers. According to the S. A. Solin group, both of the mixed metal HDS compounds $\text{Cu}_{2(1-x)}$

$\text{Zn}_{2x}(\text{OH})_3\text{X}$ ($\text{X} = \text{NO}_3^-, \text{C}_7\text{H}_{15}\text{COO}^-$) can exhibit geometric frustration with reduced magnetic order, the latter exhibiting a spin-glass-like behavior.⁶ Given that the basic ingredients of magnetic frustration behavior are frustration and spin-disorder, the reported effects of introducing non-magnetic ions on magnetic frustration are in agreement with our results. However, we believe that the key factor in the reported magnetic frustration is not the introduction of non-magnetic Zn^{2+} ions into the copper layer but rather the lattice disorder resulting from doping.

Several mixed metal HDS systems, such as Cu-Co, Co-Zn, Cu-Zn, and Ni-Zn, have been prepared through precipitation or hydrolysis.⁷ Unfortunately, magnetic studies of these systems have not yet been reported. In this paper, we report the preparation of the mixed (Cu, Ni)-HDS system, $(\text{Cu}_{0.75}\text{Ni}_{0.25})_2(\text{OH})_3\text{NO}_3$, in which the magnetic ion Ni^{2+} is substituted for some of the magnetic Cu^{2+} ions of the (Cu, Cu)-HDS system, $\text{Cu}_2(\text{OH})_3\text{NO}_3$. The crystal structures and 2D magnetic properties of (Cu, Ni)-HDS and (Cu, Cu)-HDS were also examined.

Experimental Section

The $(\text{M}_{1-x}\text{M}'_x)_2(\text{OH})_3\text{NO}_3$ systems, (M, M')-HDS, are mainly synthesized by slow hydrolysis in aqueous solution from the metal oxide, MO, and a solution of the metal nitrate, $\text{M}'(\text{NO}_3)_2$.⁸ (Cu, Cu)-HDS and (Cu, Ni)-HDS were obtained from CuO (0.2 mol) dispersed in 100 mL solutions of 0.8 M of $\text{Cu}(\text{NO}_3)_2 \cdot 3\text{H}_2\text{O}$ and $\text{Ni}(\text{NO}_3)_2 \cdot 6\text{H}_2\text{O}$, respectively. The mixtures were vigorously stirred at room temperature. After 10 days, the mixtures, which are initially black due to CuO, form grayish-green homogeneous precipitates.

The precipitates were separated from the solutions, washed with distilled water, and then air-dried.

The crystal structures of (Cu, Ni)-HDS and (Cu, Cu)-HDS were analyzed with powder X-ray diffraction (XRD, MAC Science diffractometer, MXP3A-HF) by using Cu K α radiation. The morphologies of these products were characterized with scanning electron microscopy (SEM, Leo1455VP). Fourier transform infrared (FT-IR) spectra were obtained by using a FTIR Bomem Michelson spectrometer in the transmittance mode over the range 500–4000 cm $^{-1}$ with a resolution of 4 cm $^{-1}$. The thermal properties of (Cu, Ni)-HDS and (Cu, Cu)-HDS were studied with thermogravimetric analysis (TGA, Perkin), which was performed up to 800 °C under nitrogen gas at a rate of 10 °C·min $^{-1}$. Magnetic measurements were carried out on the powdered samples enclosed in a medical cap by using a Quantum Design MPMS-7 superconducting quantum interference device (SQUID) magnetometer.

Results and Discussion

(Cu, Cu)-HDS was found to have a Mg(OH) $_2$ -type structure in which one-fourth of the OH $^-$ groups are substituted with NO $_3^-$ groups. One of the oxygen atoms of each NO $_3^-$ group is directly bonded to three copper atoms *via* Cu-O-Cu bonds. The two-dimensional structure consists of positively charged octahedral copper hydroxide layers held together by hydrogen bonds between NO $_3^-$ and OH $^-$ within the layer, displayed as orange lines in Figure 1(a). The inorganic sheets of [Cu $_2$ (OH) $_3$] $^+$ contain two distinct types of crystallographic copper sites with different oxygen environments, Cu(1) (4 OH + 2 NO $_3$) and Cu(2) (4 OH + 1 OH + 1 NO $_3$), as shown in Figure 1(b).

Figure 2 shows the X-ray diffraction patterns of (Cu, Cu)-HDS and (Cu, Ni)-HDS. (Cu, Cu)-HDS has a lamellar structure with an interlayer spacing of $d = 0.683$ nm, as is evident from the XRD patterns shown in Figure 2(a). All the XRD peaks of (Cu, Cu)-HDS are consistent with those of Cu $_2$ (OH) $_3$ NO $_3$.⁹ Since the ionic radius of the Ni $^{2+}$ ion (69 pm) is slightly smaller than that of the Cu $^{2+}$ ion (72 pm), the crystal structure of (Cu, Ni)-HDS is expected to inherit the basic framework of (Cu, Cu)-HDS with little lattice con-

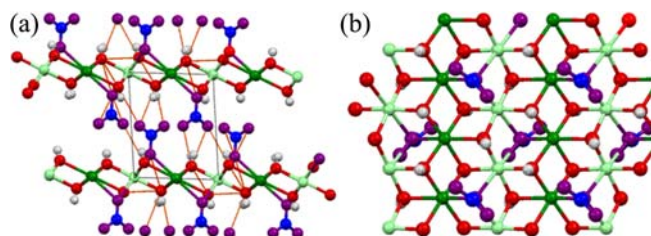


Figure 1. Crystal structure of (Cu, Cu)-HDS, Cu $_2$ (OH) $_3$ NO $_3$: viewed along (a) the b -axis and (b) the c -axis. Cu(1), Cu(2), O (from OH $^-$), O (from NO $_3^-$), N, and H are displayed as light green, green, red, violet, blue, and gray balls, respectively. The inorganic sheets of [Cu $_2$ (OH) $_3$] $^+$ contain two different types of crystallographic copper sites, Cu(1) (light green) and Cu(2) (green), with different octahedral environments.

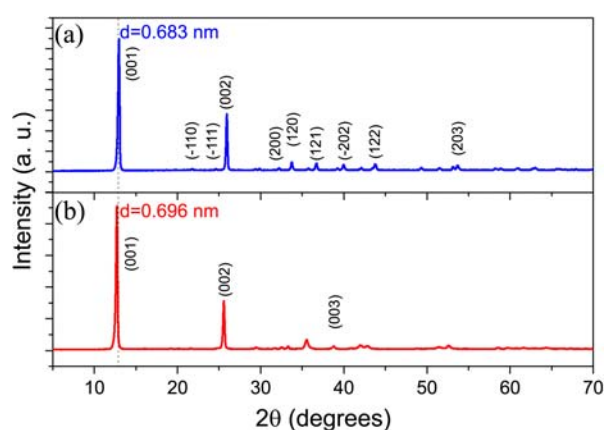


Figure 2. X-ray powder diffraction patterns and Miller indices of (a) (Cu, Cu)-HDS and (b) (Cu, Ni)-HDS.

traction because the Ni $^{2+}$ ions will occupy the copper sites in Cu $_2$ (OH) $_3$ NO $_3$. Figure 2(b) shows the XRD pattern of (Cu, Ni)-HDS, which is very similar to that of Cu $_2$ (OH) $_3$ NO $_3$. However, the basal spacing of (Cu, Ni)-HDS is slightly higher (0.696 nm) than that of (Cu, Cu)-HDS (0.683 nm). Note that the layered structures of these HDS systems are strongly dependent on hydrogen bonding between NO $_3^-$ and OH $^-$. Therefore, a slight increase in the basal spacing suggests that the nature of the M-OH $^-$ and M-NO $_3^-$ bonding in (Cu, Ni)-HDS differs from that of (Cu, Cu)-HDS; this point is discussed further below.

We used SEM to investigate the crystal morphologies and elemental compositions of (Cu, Cu)-HDS and (Cu, Ni)-HDS. Figures 3(a) and 3(b) show the SEM images of (Cu, Cu)-HDS and (Cu, Ni)-HDS, respectively. As expected, both (Cu, Cu)-HDS and (Cu, Ni)-HDS have a plate-like morphology, which is evident in the strong intensities of the (00 l) peaks in their XRD patterns. Figures 3(c) and 3(d) show the energy dispersive X-ray (EDX) spectra for (Cu, Cu)-HDS and (Cu, Ni)-HDS, respectively. For (Cu, Ni)-HDS, the mole ratio of Cu to Ni is almost equal to 3. Therefore, (Cu, Ni)-HDS has the crystal structure of Cu $_2$ (OH) $_3$ NO $_3$ and the composition (Cu $_{0.75}$ Ni $_{0.25}$) $_2$ (OH) $_3$ NO $_3$.

Figure 4 shows the TGA curves and their derivatives (DTG) for (Cu, Cu)-HDS and (Cu, Ni)-HDS. The TGA

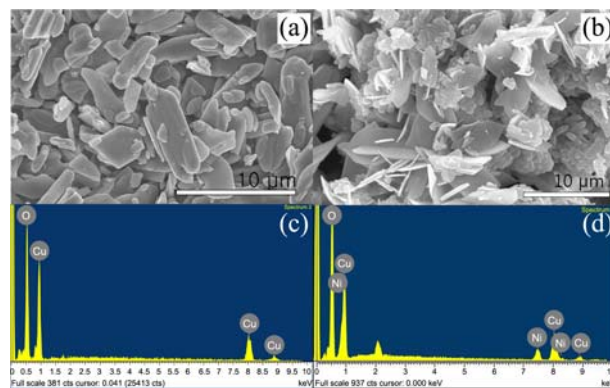


Figure 3. SEM images of (a) (Cu, Cu)-HDS and (b) (Cu, Ni)-HDS. EDX spectra of (c) (Cu, Cu)-HDS and (d) (Cu, Ni)-HDS.

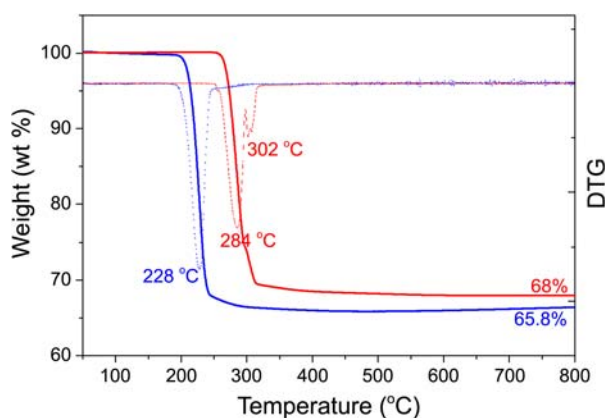


Figure 4. TGA (solid lines) and DTG curves (dotted lines) for (Cu, Cu)-HDS (blue) and (Cu, Ni)-HDS (red).

curve for (Cu, Cu)-HDS shows that there is a large mass loss at temperatures ranging from 200 to 250 °C due to decomposition into CuO. The calculated value (66.3%) of the weight percent of CuO product with respect to the (Cu, Cu)-HDS reactant agrees with the experimental value of 65.8%, which indicates that complete decomposition occurs. The TGA curve of (Cu, Ni)-HDS shows that its thermal decomposition occurs at a much higher temperature. There is a minute difference between the expected value (65.9%) and the experimental value (68.0%) for the weight percent of the mixed metal oxide product with respect to the (Cu, Ni)-HDS reactant. In general, the thermal decomposition of a HDS into the metal oxide is associated with two separate processes within a very narrow temperature range: (1) dehydroxylation of the copper hydroxide layers and (2) breaking of the N-O bond in M-O-NO₂. It is worth noting that the general trend in the decomposition temperatures of metal nitrates correlates well with the charge densities of the cations.¹⁰ According to the results of Yuvaraj *et al.*, the decomposition temperature is expected to decrease as the strength of the bond decreases.¹¹ The strength of the bond can be reduced by two main factors: (1) through polarization of the electron cloud of the nitrate anion by the charge density on the metal cation and (2) through back-donation of the nitrate electron cloud to a vacant d-orbital of the metal ion. For this reason, the decomposition temperature (290 °C) of (Ni, Ni)-HDS is higher than that of (Cu, Cu)-HDS.¹⁰ In the case of mixed metal HDS systems, thermal decomposition studies are very important for understanding the role of the mixing effect on the nature of the N-O bond in M-O-NO₂. Surprisingly, the decomposition temperature of (Cu, Ni)-HDS is very close to that of (Ni, Ni)-HDS, even though only 25% of the total number of sites for metal ions in (Cu, Ni)-HDS are occupied by nickel ions. Further, the thermal decomposition of (Cu, Ni)-HDS involves two consecutive steps near 284 and 302 °C, whereas that of (Cu, Cu)-HDS occurs near 228 °C in a single step. These differences in the thermal decomposition processes indicate that the M-NO₃ binding strengths in (Cu, Ni)-HDS are different to those in (Cu, Cu)-HDS.

FT-IR spectroscopy is an effective technique for checking

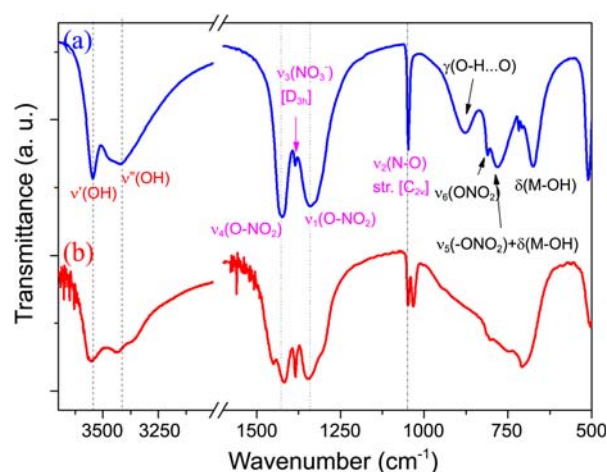


Figure 5. FT-IR spectra of (a) (Cu, Cu)-HDS and (b) (Cu, Ni)-HDS.

the bonding nature and presence of nitrate and hydroxide anions. It is well known that the number and positions of the absorption bands of NO₃⁻ depend on the coordination environment of the nitrate ligand.¹² Our comparison of the observed IR absorptions with the frequencies of monodentate NO₃ groups in transition metal nitrates enabled us to assign the absorptions at 1485-1415, 1340-1305, and 1046-968 cm⁻¹ to the ν₄, ν₁, and ν₂ fundamentals, which correspond to asymmetric stretching, symmetric stretching of the O-NO₂ mode, and symmetric stretching of the N-O mode for monodentate nitrate with C_{2v} site symmetry, respectively.¹³ Figure 5 shows the FT-IR spectra of (Cu, Cu)-HDS and (Cu, Ni)-HDS, and their spectral assignments are presented in Table 1.

The clearest differences between the spectra of (Cu, Cu)-HDS and (Cu, Ni)-HDS are associated with the double split of the ν₄ and ν₂ modes (with C_{2v} site symmetry) and with the increase in the intensity of the ν₃ mode (with D_{3h} site symmetry) of the nitrate anion. The frequency shift of the ν₂ mode and the splitting, Δν (= ν₄-ν₁), have been shown to

Table 1. FT-IR data for (Cu, Cu)-HDS and (Cu, Ni)-HDS and their spectral assignments

Wavenumber (cm ⁻¹)		Assigned modes
(Cu, Cu)-HDS	(Cu, Ni)-HDS	
3545	3550	ν(O-H...O) ¹ : asymmetric OH stretching
3421	3436	ν(O-H...O) ² : symmetric OH stretching
1423	1448, 1417	ν ₄ (O-NO ₂): asymmetric stretching [C _{2v}]
1385	1384	ν ₃ (NO ₃ ⁻): absorption band [D _{3h}]
1338	1347	ν ₁ (O-NO ₂): symmetric stretching [C _{2v}]
1047	1048, 1033	ν ₂ (N-O): stretching [C _{2v}]
876		γ(O-H...O): bending
810	802	ν ₆ (ONO ₂)
781	747	ν ₃ (-ONO ₂) + δ(M-OH)
717		ν ₃ (-ONO ₂)
708	708	
675		δ(M-OH): bending
511	504	

vary with the degree of covalent character of the M-ONO₂ bond.¹⁴ In the case of (Cu, Ni)-HDS, one of the ν_2 modes with a double split is silent but the other is shifted lower. Moreover, the splitting values of $\Delta\nu$ ($=\nu_4-\nu_1$) are 101 and 70 cm^{-1} due to the doubly split ν_4 mode, which suggest that there are two different strengths of bonding interactions between NO₃ and the metal cations. In addition, the two asymmetric and symmetric OH stretching bands of the hydroxy groups in (Cu, Ni)-HDS are observed at a higher frequency, which indicates that there is a lower level of hydrogen bonding. From our detailed analysis of the XRD and TGA patterns and the FT-IR spectra, we conclude that the crystal structure of (Cu, Ni)-HDS resembles that of (Cu, Cu)-HDS but that subtle changes in the mixed metal-NO₃ bonding character of (Cu, Ni)-HDS accompanied by the reduced level of hydrogen bonding between OH...NO₃⁻ give rise to an increase in its interlayer spacing.

The (Cu, Cu)-HDS system, Cu₂(OH)₃NO₃, is well known to have the structure of the 2D Heisenberg antiferromagnetic (AFM) model compound with a triangular magnetic lattice, as shown in Figure 1(b).¹⁵ There are many kinds of magnetic pathways within the inorganic layer, *via* Cu(1)-O-Cu(1), Cu(2)-O-Cu(2), Cu(1)-O-Cu(2) and so on. The competition between magnetic interactions through different pathways

within a triangular lattice gives rise to magnetic frustration in HDS systems. However, the (Cu, Cu)-HDS system exhibits no magnetic frustration that will be expected 2D triangular lattice. The influence on the magnetic properties of (Cu, Cu)-HDS of substitution of some of the copper sites with magnetic Ni²⁺ ions is very important for understanding the low-dimensional magnetism involving spin-frustration. The temperature dependences of the magnetic susceptibility (χ_{mol}) and the magnetic susceptibility temperature product ($\chi_{\text{mol}}T$) for (Cu, Cu)-HDS and (Cu, Ni)-HDS were measured over the temperature range 5-300 K in an applied field of 10 kOe, and are presented in Figure 6. In the case of (Cu, Cu)-HDS, the magnetic susceptibility, χ_{mol} , increases with decreasing temperature, reaching a broad maximum of 0.0532 $\text{cm}^3\cdot\text{mol}^{-1}$ at approx. 12 K, and then decreases to a value of 0.0368 $\text{cm}^3\cdot\text{mol}^{-1}$ at 5 K. A broad maximum for (Cu, Cu)-HDS was detected, which is usually seen in low-dimensional antiferromagnets.¹⁶ The high temperature data above 150 K can be fitted very well with the Curie-Weiss law, $\chi_{\text{mol}} = C/(T-\theta)$, as displayed in Figure 6(a), with $C = 0.9723 \text{ cm}^3\cdot\text{mol}^{-1}\cdot\text{K}$ and $\theta = -0.5404 \text{ K}$, which suggests that there are weak intralayer AFM interactions. When some Cu²⁺ ions are substituted with Ni²⁺ ions, the magnetic behaviors are totally different: the magnetic susceptibility (χ_{mol}) of (Cu, Ni)-HDS is generally inversely proportional to temperature with no broad maximum. The magnetic data above 200 K can also be fitted with the Curie-Weiss law with $C = 1.4355 \text{ cm}^3\cdot\text{mol}^{-1}\cdot\text{K}$ and $\theta = -4.7390 \text{ K}$, which indicates that there is strong intralayer AFM coupling. In general, the maximum in the susceptibility of AFM materials arises at a temperature known as the Neel temperature in the low temperature region. In addition to the absence of a broad maximum in χ_{mol} , (Cu, Ni)-HDS exhibits stronger intralayer AFM coupling. Furthermore, their slopes are steeper than predicted by the Curie-Weiss law, which suggests the presence of ferromagnetic (FM) interactions.¹⁷

To clarify the differences between the magnetic behaviors of (Cu, Cu)-HDS and (Cu, Ni)-HDS, the temperature dependences of $\chi_{\text{mol}}T$ for (Cu, Cu)-HDS and (Cu, Ni)-HDS are displayed in Figure 6(b). At high temperatures, the $\chi_{\text{mol}}T$ values of (Cu, Cu)-HDS are equivalent to two Cu(II) (d^9 , $S = 1/2$) per mole (approx. 0.8 $\text{cm}^3\cdot\text{mol}^{-1}\cdot\text{K}$). The $\chi_{\text{mol}}T$ of (Cu, Cu)-HDS decreases smoothly with decreasing temperature, finally approaching zero, which indicates the presence of AFM interactions. The temperature dependence of $\chi_{\text{mol}}T$ for (Cu, Ni)-HDS is more complex. The $\chi_{\text{mol}}T$ values increase slightly with decreasing temperature in the temperature range 200 K to 20 K, which is clearly indicative of dominant FM intralayer interactions, reaching a maximum at approx. 20 K. $\chi_{\text{mol}}T$ decreases sharply as the temperature is further decreased, which suggests that there are AFM interlayer interactions. The high $\chi_{\text{mol}}T$ value of 1.42 $\text{cm}^3\cdot\text{mol}^{-1}\cdot\text{K}$ at 300 K indicates the coexistence of Cu(II) (d^9 , $S = 1/2$) and Ni(II) (d^8 , $S = 1$).

The magnetic properties of (Cu, Ni)-HDS are quite different from those of (Cu, Cu)-HDS. In-plane short-range FM interactions occur in (Cu, Ni)-HDS at higher temperatures,

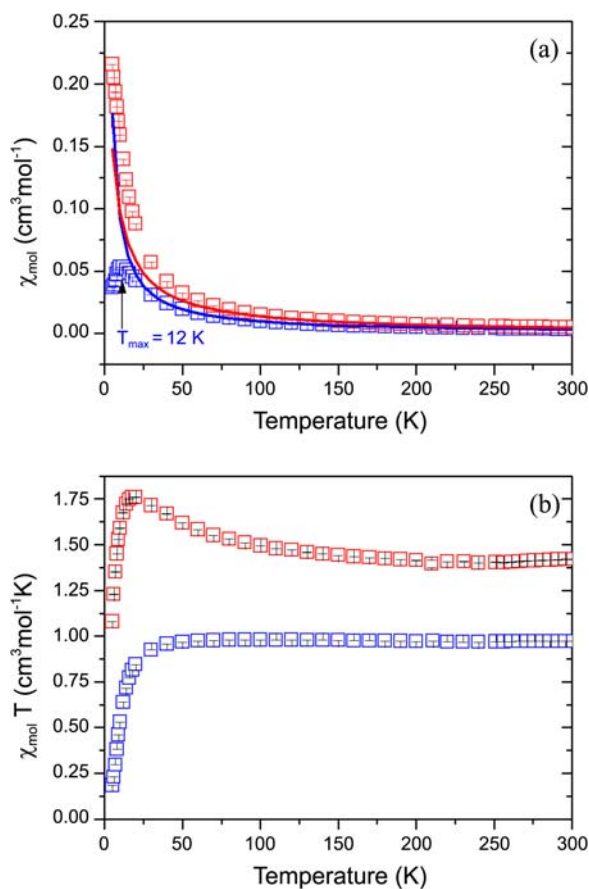


Figure 6. Temperature dependences of (a) the molar magnetic susceptibility (χ_{mol}) and (b) the magnetic susceptibility temperature product ($\chi_{\text{mol}}T$) for (Cu, Cu)-HDS (blue) and (Cu, Ni)-HDS (red). The lines are the best-fit curves to the Curie-Weiss law.

and strong long-range AFM interactions are present below 20 K. The magnetic anisotropy of (Cu, Ni)-HDS can be attributed to the coexistence of distinct FM and AFM in-plane interactions. The various in-plane magnetic interactions stem from the different magnetic exchange pathways *via* M(1)-O-M(1), M(2)-O-M(2), M(1)-O-M(2) that are created by the introduction of Ni²⁺ ions into the (Cu, Cu)-HDS framework. It is worth noting that the magnetic properties of HDS are governed by the characteristics of the in-plane magnetic interactions and can thus be tuned by the doping of magnetic sites. From these results, we conclude that magnetic anisotropy can be achieved in HDS systems by doping with a magnetic ion, which in turn gives rise to an increase in the spin-disorder in the magnetic lattice. The magnetic doping of the copper sites in (Cu, Cu)-HDS has a strong influence on the interlayer structure, the bonding nature of M-NO₃⁻, and on the thermal and magnetic properties of the material. A systematic investigation of the effects of the doping of HDS systems on their crystal structures, bonding nature, and magnetic properties is underway.

Conclusions

(Cu, Cu)-HDS and (Cu, Ni)-HDS were prepared with the slow hydrolysis method in order to investigate their 2D magnetic properties. According to our XRD results, the two HDS samples have typical layered structures with different interlayer distances. The difference between their interlayer distances originates from differences in the M-NO₃⁻ bonding nature within the layers, which result in different thermal decomposition behaviors and significantly different magnetic properties. (Cu, Cu)-HDS exhibits AFM interactions throughout the entire temperature range, whereas (Cu, Ni)-HDS exhibits in-plane short-range FM interactions at high temperatures and long-range AFM interactions between the layers below 20 K.

Acknowledgments. This research was supported by the National Research Foundation of Korea funded by the Ministry of Education, Science, and Technology (KRF-2011-0018589).

References

- (a) Clearfield, A. *Prog. Inorg. Chem.* **1998**, *47*, 371. (b) Cao, G.; Hong, H. G.; Mallouck, T. E. *Acc. Chem. Res.* **1992**, *25*, 420. (c) Arizaga, G. G. C.; Satynarayana, K. G.; Wypych, F. *Solid State Ionics* **2007**, *178*, 1143.
- Park, S. H.; Kim, H. J. *J. Am. Chem. Soc.* **2004**, *126*, 14368.
- de Jong, J. J. *Magnetic Properties of Layered Transition Metal Complexes*; Kluwer Academic Publishers: Dordrecht, 1990.
- (a) Girtu, M. A.; Wynn, C. M.; Fujita, W.; Awaga, K.; Epstein, A. *J. Phys. Rev. B* **2000**, *61*, 4117. (b) Rogez, G.; Massobrio, C.; Rabu, P.; Drillon, M. *Chem. Soc. Rev.* **2011**, *40*, 1031.
- (a) Fujita, W.; Awaga, K. *Inorg. Chem.* **1996**, *35*, 1915. (b) Rabu, P.; Rouba, S.; Laget, V.; Hornick, C.; Drillon, M. *Chem. Commun.* **1996**, 1107. (c) Kurmoo, M.; Day, P.; Derory, A.; Estournès, C.; Poinso, R.; Stead, M. J.; Kepert, C. J. *J. Solid State Chem.* **1999**, *145*, 452. (d) Park, S. H.; Lee, C. H.; Lee, C. E.; Ri, H. C.; Shim, S. Y. *Mater. Res. Bull.* **2002**, *37*, 1773. (e) Park, S. H.; Lee, C. E. *J. Phys. Chem. B* **2005**, *109*, 1118. (f) Park, S. H.; Lee, C. E. *Bull. Korean Chem. Soc.* **2006**, *27*, 1587.
- (a) Wu, J.; Gangopadhyay, A. K.; Kanjanaboos, P.; Solin, S. A. *J. Phys.: Condens. Matter* **2010**, *22*, 334211. (b) Wu, J.; Wilderboer, J. S.; Werner, F.; Seidel, A.; Nussinov, Z.; Solin, S. A. *Europhys. Lett.* **2011**, *93*, 67001.
- (a) Zotov, N.; Petrov, K.; Dimitrova-Pankova, M. *J. Phys. Chem. Solids* **1990**, *51*, 1199. (b) Petrov, K.; Zotov, N.; Mirtcheva, E.; García-Martínez, O.; Rojas, R. M. *J. Mater. Chem.* **1994**, *4*, 611. (c) Atanasov, M.; Petrov, K.; Mirtcheva, E.; Friebel, C.; Reinen, D. *J. Solid State Chem.* **1995**, *118*, 303. (d) Choy, J. H.; Kwon, Y. M.; Han, K. S.; Song, S. W.; Chang, S. H. *Mater. Lett.* **1998**, *34*, 356. (e) Rojas, R.; Barriga, C.; Ulibarri, M. A.; Malet, P.; Rives, V. *J. Mater. Chem.* **2002**, *12*, 1071. (f) Izaoumen, N.; Cherrab, M.; Rissouli, K.; Benkhouja, K.; Jaafari, K.; Fahad, M. *J. Phys. IV France* **2005**, *123*, 291. (g) Rajamathi, J. T.; Raviraj, N. H.; Ahmed, M. F.; Rajamathi, M. *Solid State Sci.* **2009**, *11*, 2080.
- Meyn, M.; Beneke, K.; Lagaly, G. *Inorg. Chem.* **1993**, *32*, 1209.
- Oswald, H. R. *Z. Kristallogr.* **1961**, *116*, 210.
- Biswick, T.; Jones, W.; Pacula, A.; Serwicka, E. *J. Solid State Chem.* **2006**, *179*, 49.
- Yuvaraj, S.; Fan-Yuan, L.; Tsong-Huei, C.; Chuin-Tih, Y. *J. Phys. Chem. B* **2003**, *107*, 1044.
- (a) Addison, C. C.; Gatehouse, B. M. *J. Chem. Soc.* **1960**, 613. (b) Gatehouse, B. M.; Livingstone, S. E.; Nyholm, R. S. *J. Chem. Soc.* **1957**, 505.
- Nakamoto, K. *Infrared and Raman Spectra of Inorganic and Coordination Compounds*, 5th ed.; John Wiley & Sons: New York, 1997.
- Chouillet, C.; Krafft, J. M.; Louis, C.; Lauron-Pernot, H. *Spectrochim. Acta A* **2004**, *60*, 505.
- Ruiz, E.; Lluell, M.; Cano, J.; Rabu, P.; Drillon, M.; Massobrio, C. *J. Phys. Chem. B* **2006**, *110*, 115.
- (a) Blake, A. B.; Hatfield, W. E. *J. Chem. Soc., Dalton Trans.* **1979**, 1725. (b) Park, S. H.; Oh, I. H.; Park, S.; Park, Y.; Kim, J. H.; Huh, Y. D. *Dalton Trans.* **2012**, *41*, 1237.
- Miller, J. S.; Epstein, A. J. *Angew. Chem. Int. Ed.* **1994**, *33*, 385.